

## Mechanism of the Photodissociation of 4-Diphenyl(trimethylsilyl)methyl-*N,N*-dimethylaniline

Dimitrios A. Tasis,<sup>1,†</sup> Michael G. Siskos,<sup>†</sup> Antonios K. Zarkadis,<sup>\*,†</sup> Steen Steenken,<sup>‡</sup> and Georgios Pistolis<sup>§</sup>

Department of Chemistry, University of Ioannina, 451 10 Ioannina, Greece, Max-Planck-Institut für Strahlenchemie, 45470 Mülheim, Germany, and N.C.S.R, "Democritos", 15310 Aghia Paraskevi, Attiki, Greece

azarkad@cc.uoi.gr

Received January 10, 2000

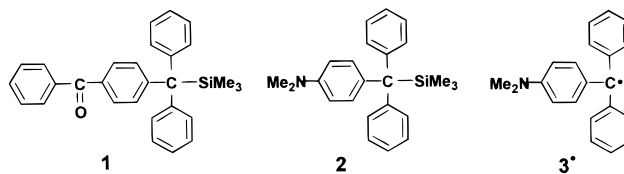
On irradiation in hexane (248- and 308-nm laser light) 4-diphenyl(trimethylsilyl)methyl-*N,N*-dimethylaniline, **2**, undergoes photodissociation of the C–Si bond giving 4-*N,N*-dimethylaminotriphenylmethyl radical, **3**<sup>•</sup> ( $\lambda_{\text{max}}$  at 343 and 403 nm), in very high quantum yield ( $\Phi = 0.92$ ). The intervention of the triplet state of **2** ( $\lambda_{\text{max}}$  at 515 nm) is clearly demonstrated through quenching experiments with 2,3-dimethylbuta-1,3-diene, styrene, and methyl methacrylate using nanosecond laser flash photolysis (LFP). The formation of **3**<sup>•</sup> is further demonstrated using EPR spectroscopy. The detection of the S<sub>1</sub> state of **2** was achieved using 266-nm picosecond LFP, and its lifetime was found to be 1400 ps, in agreement with the fluorescence lifetime ( $\tau_f = 1500$  ps,  $\Phi_f = 0.085$ ). The S<sub>1</sub> state is converted almost exclusively to the T<sub>1</sub> state ( $\Phi_T = 0.92$ ). In polar solvents such as MeCN, **2** undergoes (1) photoionization to its radical cation **2**<sup>•+</sup>, and (2) photodissociation of the C–Si bond, giving radical **3**<sup>•</sup> as before in hexane. The formation of **2**<sup>•+</sup> occurs through a two-photon process. Radical cation **2**<sup>•+</sup> does not fragment further, as would be expected, to **3**<sup>•</sup> via a nucleophile(MeCN)-assisted C–Si bond cleavage but regenerates the parent compound **2**. Obviously, the bulkiness of the triphenylmethyl group prevents interaction of **2**<sup>•+</sup> with the solvent (MeCN) and transfer to it of the electrofugal group Me<sub>3</sub>Si<sup>+</sup>. The above results of the laser flash photolysis are supported by pulse radiolysis, fluorescence measurements, and product analysis.

### Introduction

Photodissociation represents one of the most important key steps in photochemical processes. In photopolymerization reactions, for example, the photoinitiator, being a chromophoric system, is able to undergo efficient photodissociation giving free radicals that subsequently trigger the polymerization reaction.<sup>2</sup>

Whereas benzyltrimethylsilane PhCH<sub>2</sub>-SiMe<sub>3</sub> has been described<sup>3,4</sup> as nearly photochemically inert under direct irradiation, introduction of chromophore groups such as the anilino group on the benzylic carbon<sup>5</sup> or the benzoyl group<sup>6</sup> on the aromatic ring considerably enhances its

ability to undergo C–Si bond cleavage with formation of benzyl and Me<sub>3</sub>Si<sup>•</sup> radicals. Moreover, phenyl substitution on the benzylic carbon leads to a weakening of the C–Si bond, which further facilitates its photocleavage, as has been found for similar systems.<sup>7,8</sup> Compound **1** is such a system,<sup>7</sup> and we showed recently that its photofragmen-



tation efficiency sharply increases relative to PhCH<sub>2</sub>-SiMe<sub>3</sub>, giving *p*-(benzoyl)triphenylmethyl radical with a high quantum yield (~0.9). Compound **1** proved to be a good photoinitiator for the polymerization of methyl methacrylate and styrene.<sup>9</sup> The very reactive radical Me<sub>3</sub>-Si<sup>•</sup><sup>10</sup> produced by the photodissociation of the C–Si bond adds to the monomer double bond, thus initiating the polymerization.<sup>9</sup> In the past, the highly toxic Hg(SiMe<sub>3</sub>)<sub>2</sub>

\* Tel: (+30 651) 98379, 98398. Fax: (+30 651) 98799. E-mail: azarkad@cc.uoi.gr.

<sup>†</sup> University of Ioannina.

<sup>‡</sup> Max-Planck-Institut für Strahlenchemie.

<sup>§</sup> N.C.S.R, "Democritos".

(1) Tasis, D. Ph.D. Thesis, University of Ioannina, in preparation. Siskos, M. G.; Tasis, D. A.; Zarkadis, A. K.; Steenken, S. *37th IUPAC International Chemical Congress*, Berlin, 14–19 August 1999.

(2) Allen, N. S. *Photopolymerization and Photoimaging Science and Technology*; Elsevier Applied Science: London, 1989. Scranton, A. B.; Bowman, C. N.; Peiffer, R., Eds.; *Photopolymerization: Fundamentals and Applications*; ACS Symposium Series 673; American Chemical Society: Washington, DC, 1997.

(3) Valkovich, P. B.; Ito, T. I.; Weber, W. P. *J. Org. Chem.* **1974**, *39*, 3543.

(4) (a) Kira, M.; Yoshita, H.; Sakurai, H. *J. Am. Chem. Soc.* **1985**, *107*, 7767. Sakurai, H.; Yoshita, H.; Kira, M. *J. Chem. Soc., Chem. Com.* **1985**, 1780. (b) A very low quantum yield of PhCH<sub>2</sub><sup>•</sup> ( $\Phi = 0.07$ ) generated by the photolysis of PhCH<sub>2</sub>SiMe<sub>3</sub> in MeOH has been reported in a recent paper.<sup>4c</sup> (c) Hiratsuka, H.; Kobayashi, S.; Minegishi, T.; Hara, M.; Okutsu, T.; Murakami, S. *J. Phys. Chem. A* **1999**, *103*, 9174.

(5) Siskos, M. G.; Garas, S. K.; Zarkadis, A. K.; Bokaris, E. P. *Chem. Ber.* **1992**, *125*, 2477.

(6) Georgakilas, V. Ph.D. Thesis, University of Ioannina, 1998. Zarkadis, A. K.; Siskos, M. G.; Georgakilas, V.; Steenken, S.; Karakostas, N.; Garas, S. K. *XVIIIth International Conference on Photochemistry*, Warsaw, August 3–8, 1997.

(7) Hillgartner, H.; Neumann, W. P.; Schulten, W.; Zarkadis, A. K. *J. Organomet. Chem.*, **1980**, *201*, 197.

(8) (a) Siskos, M. G.; Zarkadis, A. K.; Steenken, S.; Karakostas, N.; Garas, S. K. *J. Org. Chem.* **1998**, *63*, 251. (b) Siskos, M. G.; Zarkadis, A. K.; Steenken, S.; Karakostas, N. *J. Org. Chem.* **1999**, *64*, 1925.

(9) Tasis, D. A.; Siskos, M. G.; Zarkadis, A. K. *Macromol. Chem. Phys.* **1998**, *199*, 1981.

has been used as a source of  $\text{Me}_3\text{Si}^{\cdot}$  radicals for the photopolymerization of styrene.<sup>11</sup> Di- and polysilanes<sup>12,13</sup> that form silyl radicals photochemically have also been used.

These findings prompted us to examine the photochemical behavior of an analogous system **2**. We essentially replaced the benzophenone chromophore by the dimethylanilino group, which possesses a higher excitation energy.<sup>14</sup> Increase of the excited state energy should more readily lead to photodissociation<sup>15</sup> and formation of the stabilized radical **3**<sup>•</sup> and the very reactive (against ethylenic monomers)  $\text{Me}_3\text{Si}^{\cdot}$  radical. The latter is a good initiator in polymerization reactions, as we showed earlier using **1**.<sup>9</sup>

On the other hand, the dimethylanilino chromophore, as a result of its low ionization potential, introduces an additional complication to the system: the tendency to photoionize in polar solvents, giving the corresponding radical cation.<sup>16</sup> However, radical ions are very reactive intermediates and in general undergo very efficient fragmentation in solution, generating a radical and a cation.<sup>17</sup> Especially, in the case of benzyltrimethylsilane derivatives, numerous investigations<sup>18</sup> focus on their photooxidation, which affords the corresponding radical

(10) The  $\text{Me}_3\text{Si}^{\cdot}$  radical is known to undergo very fast additions to olefinic bonds ( $k \approx 10^7\text{--}10^9 \text{ M}^{-1}\text{s}^{-1}$ ); see: Chatgililoglu, C. *Chem. Rev.* **1995**, *95*, 1229. Chatgililoglu, C.; Ingold, K. U.; Scaiano, J. C. *J. Am. Chem. Soc.* **1983**, *105*, 3292. Choo, K. Y.; Gaspar, P. P. *J. Am. Chem. Soc.* **1974**, *96*, 1248. Jackson, R. A. *J. Chem. Soc., Chem. Commun.* **1974**, 573.

(11) Hisayoshi, I.; Yozo, M.; Masayoshi, K. *Macromol. Chem.* **1976**, *177*, 2647.

(12) Woo, H. G.; Park, S. H.; Park, J. Y.; Yang, S. Y.; Ham, H. S.; Kim, W. G. *Bull. Korean Chem. Soc.* **1996**, *17*, 373.

(13) Alonso, A.; Peinado, C.; Lozano, A. E.; Catalina, F.; Zimmermann, C.; Schnabel, W. *J. Macromol. Sci., Pure Appl. Chem.* **1999**, *A36*, 605. Miller, R. D.; Michl, J. *Chem. Rev.* **1989**, *89*, 1359. West, R.; Wolff, A. R.; Peterson, D. J. *J. Rad. Curing* **1986**, *13*, 35. Yücesan, D.; Hostoygar, H.; Denizligil, S.; Yagci, Y. *Angew. Makromol. Chem.* **1994**, *221*, 207. Chen, H. B.; Chang, T. C.; Chiu, Y. S.; Ho, S. Y. *J. Polym. Sci., Polym. Chem. Ed.* **1996**, *34*, 679. Semenov, V. V.; Cherepennikova, N. F.; Artmicheva, S. B.; Razuvaev, G. A. *Appl. Organomet. Chem.* **1990**, *4*, 163.

(14) Benzophenone,  $E_{\text{triplet}} = 68 \text{ kcal/mol}$ ; dimethylaniline,  $E_{\text{singlet}} = 91.5 \text{ kcal/mol}$  in nonpolar solvents,  $89.6 \text{ kcal/mol}$  in polar solvents and  $E_{\text{triplet}} = 75.8 \text{ kcal/mol}$  in polar solvents; see: Murov, S. L.; Carmichael, I.; Hug, G. L. *Handbook of Photochemistry*, 2nd ed.; Marcel Dekker: New York, 1993.

(15) Michl, J.; Bonacic-Koutecky, V. *Electronic Aspects of Organic Photochemistry*; Wiley-Interscience: New York, 1990; pp 138, 292, 374.

(16) (a) Malkin, J. *Photochemical and Photophysical Properties of Aromatic Compounds*; CRC: Boca Raton, FL, 1992; pp 117, 201. (b) Malkin, Ya. N.; Kuz'min, V. A. *Russ. Chem. Rev.* **1985**, *54*, 1041. (c) Saito, F.; Tobita, S.; Shizuka, H. *J. Photochem. Photobiol. A* **1997**, *106*, 119. (d) Saito, F.; Tobita, S.; Shizuka, H. *J. Chem. Soc., Faraday Trans.* **1996**, *92*, 4177. (e) McKellar, J. F. *Photochem. Photobiol.* **1967**, *6*, 287.

(17) (a) Arnold, D. R.; Maroulis, A. G. *J. Am. Chem. Soc.* **1976**, *98*, 5931. (b) Popielarz, R.; Arnold, D. R. *J. Am. Chem. Soc.* **1990**, *112*, 3068. (c) Arnold, D. R.; Du, X.; Chen, J. *Can. J. Chem.* **1995**, *73*, 307. (d) Reichel, L. W.; Griffin, G. W. *J. Am. Chem. Soc.* **1984**, *106*, 6968. (e) Malsak, P.; Chapman, H., Jr.; Vallombroso, T. M., Jr.; Watson, B. A. *J. Am. Chem. Soc.* **1995**, *117*, 12380. (f) Gaillard, E. R.; Whitten, D. G. *Acc. Chem. Res.* **1996**, *29*, 292. (g) Burton, R. D.; Bartberger, M. D.; Zhang, Y.; Eyley, J. R.; Schanze, K. S. *J. Am. Chem. Soc.* **1996**, *118*, 5655. (h) Albin, A. L. W.; Siviero, E.; Mella, M.; Long, C.; Pratt, A. *J. Chem. Soc., Perkin Trans. 2* **1995**, 1895. (i) Su, Z.; Mariano, P. S.; Falvey, D. E.; Yoon, U. C.; Oh, S. W. *J. Am. Chem. Soc.* **1998**, *120*, 10676.

(18) (a) Dinnocenzo, J. P.; Farid, S.; Goodman, J. L.; Gould, I. R.; Todd, W. R.; Mattes, S. L. *J. Am. Chem. Soc.*, **1989**, *111*, 8973. (b) Dockery, K. P.; Dinnocenzo, J. P.; Farid, S.; Goodman, J. L.; Gould, I. R.; Todd, W. R. *J. Am. Chem. Soc.* **1997**, *119*, 1876. (c) Freccero, M.; Pratt, A.; Albin, A.; Long, C. *J. Am. Chem. Soc.* **1998**, *120*, 284. (d) Mella, M.; Fagnoni, M.; Freccero, M.; Fasani, E.; Albin, A. *Chem. Soc. Rev.* **1998**, *27*, 81. (e) Baciocchi, E.; Del Giacco, T.; Rol, C.; Sebastiani, G. V. *Tetrahedron Lett.* **1989**, *30*, 3573. (f) Baciocchi, E.; Del Giacco, T.; Elisei, F.; Ioele, M. *J. Org. Chem.*, **1995**, *60*, 7974. (g) Dinnocenzo, J. P.; Farid, S.; Goodman, J. L.; Gould, I. R.; Todd, W. P. *Mol. Cryst. Liq. Cryst.* **1991**, *194*, 151.

cation. The latter may subsequently transfer the electrofugal group  $\text{Me}_3\text{Si}^+$  to the solvent (MeCN) or to another nucleophilic reagent present in the medium, giving finally benzyl radicals.

In this paper we present an investigation of the photochemical and photophysical behavior of **2** using nanosecond and picosecond laser flash photolysis (LFP) and explore its potential as a photoinitiator with styrene and methyl methacrylate. The results are also supported by pulse radiolysis, EPR spectroscopy, fluorescence, and product analysis.

## Experimental Section

**Materials.** The synthesis of compound **2** has been described previously.<sup>5</sup> Acetonitrile, hexane, cyclohexane, propanol-2 (Merck), and *n*-BuCl (Fluka) were spectroscopic grade and used as received.

**Methods.** Fluorescence emission and excitation spectra were obtained on a Edinburgh FS900 spectrofluorimeter. Fluorescence quantum yields were measured by comparison with the reported values for aniline ( $\Phi_f = 0.17^{19}$  and  $0.11^{20}$  in cyclohexane with excitation wavelengths  $\lambda_{\text{ex}} = 290$  and  $254$  nm, respectively, and  $\Phi_f = 0.15^{21}$  in MeCN with excitation wavelength  $\lambda_{\text{ex}} = 290$  nm). Fluorescence lifetimes were measured using a time-correlated single-photon counter. The samples were excited with a spark lamp (PRA 510C), filled with hydrogen gas (0.6 bar) and operated at 6 kV.

Electron paramagnetic resonance spectra were obtained on a Varian E-109 spectrometer. The EPR tube was irradiated with a Heraeus TNN 15/32 W low-pressure lamp and then was transferred to the cavity of EPR. Gas chromatographic analyses and separations were conducted on a Hewlett-Packard 5890, Series II, FID gas chromatograph with an OV-1701, 15 m capillary column and a Siemens 1 mV recorder (injector,  $200^\circ\text{C}$ ; detector,  $300^\circ\text{C}$ ; column temperature,  $70\text{--}280^\circ\text{C}$ ,  $8^\circ\text{C}/\text{min}$ ). GC-MS analyses were performed on a SSQ 700, EI instrument with the same column as above and under identical conditions.

**Photochemical Experiments (Product Analyses).** The samples were irradiated using a 248-nm (KrF\*) or a 308-nm (XeCl\*) excimer laser at  $20^\circ\text{C}$  or a Philips HPK-125 W medium-pressure mercury vapor quartz lamp in special quartz cuvettes. The photolysis solutions were in all cases purged with argon before irradiation.

**Nanosecond and Picosecond Laser Flash Photolysis Experiments.** The solutions ( $A/\text{cm}$  ca. 0.8–1.6) were deoxygenated by bubbling with argon and photolyzed at  $20^\circ\text{C}$  in a flow system (Suprasil quartz cell) using 20-ns pulses (0.3–100 mJ) of 248 nm light (KrF\*) from a Lambda Physik EMG 103MSC excimer laser or 308-nm light (XeCl\*) from a Lambda Physik EMG150E laser. The time-dependent optical absorption signals of the transients were digitized simultaneously by Tektronix 7612 and 7912 transient recorders interfaced with a DEC LSI 11/73+ computer, which also was used for process control of the apparatus and performed on-line analysis of the experimental data.

The transient picosecond spectrometer ("pump-probe" technique) was based on a mode-locked Nd:YAG laser (PY61C-10, Continuum):  $\lambda = 1.064 \mu\text{m}$ , pulse width of 30 ps, pulse repetition rate of 10 Hz, single pulse energy  $E = 40$  mJ. As pump beam the excitation wavelengths  $\lambda_{\text{exc}} = 266$  nm and as a probe beam the white light continuum ( $\lambda = 420\text{--}900$  nm) generated in the flow cell with  $\text{D}_2\text{O}$  were used. The angle between the excitation and probing white light continuum beams was  $90^\circ$ . The accumulation over 100 pulses allowed for the changes in absorbance to reach the sensitivity level of  $\leq 0.01$ .

(19) Perichet, G.; Chapelon, R.; Pouyet, B. *J. Photochem.* **1980**, *13*, 67.

(20) Malkin, Ya. N.; Ruziev, Sh.; Pigorov, N. O.; Kuz'min, V. A. *Bull. Akad. USSR, Ser. Chem.* **1987**, *36*, 51.

(21) Köhler, G. *J. Photochem.* **1987**, *38*, 217.

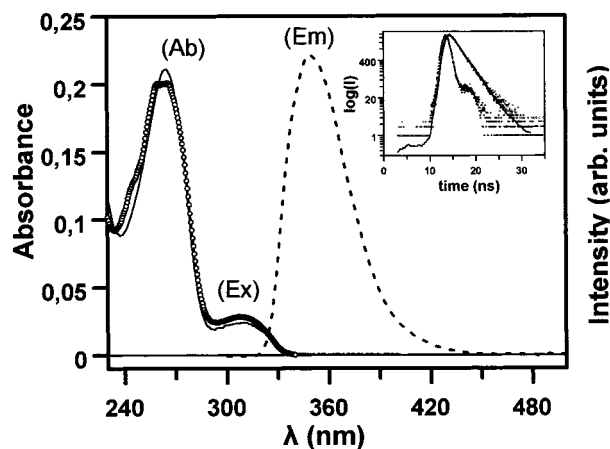


**Figure 1.** Absorption (Ab), fluorescence (Em), and fluorescence excitation (Ex) spectra of **2** in cyclohexane at 298 K,  $\lambda_{\text{ex}}$  at 290 nm. Inset: fluorescence decay trace and best-fitting curve ( $8 \times 10^{-6}$  M in cyclohexane; lower curve, lamp profile  $\lambda_{\text{ex}} = 290$  nm).

**Table 1. Absorption ( $\nu_{\text{a}}^{\text{max}}$ ) and Fluorescence ( $\nu_{\text{f}}^{\text{max}}$ ) Peaks of the Aniline and **2**, Fluorescence Lifetime ( $\tau_{\text{f}}$ ), and Fluorescence Quantum Yield ( $\Phi_{\text{f}}$ ) in Cyclohexane (CH) and MeCN at 25 °C**

sample solvent	$\nu_{\text{a}}^{\text{max}}$ ( $10^3 \text{ cm}^{-1}$ )		$\Delta\nu$ ( $10^3 \text{ cm}^{-1}$ )	$\tau_{\text{f}}$ (ns)	$\Phi_{\text{f}}$ at $\lambda_{\text{ex}} = 290$ nm ( $\lambda_{\text{ex}} = 254$ nm)
	${}^1\text{L}_{\text{a}} \leftarrow {}^1\text{A}$	${}^1\text{L}_{\text{b}} \leftarrow {}^1\text{A}$			
aniline CH	42.74 (234) <sup>a</sup> 34.82 (287)	31.08 (322) <sup>a</sup>	3.74	2.93	0.17 (0.11)
aniline MeCN	41.89 (239) 34.65 (289)	29.94 (334)	4.71		0.15
<b>2</b> CH	37.88 (264) 32.40 (309)	28.65 (349)	3.75	1.5	0.085 (0.075)
<b>2</b> MeCN	37.49 (267) 32.49 (308)	27.51 (364)	5.18		0.108

<sup>a</sup> The values in parentheses are in nm.

**Pulse Radiolysis Experiments.** A 3-MeV van der Graaf electron accelerator was used as radiation source. The detection system was similar to that described for the laser. A 20 mm  $\times$  10 mm suprasil quartz cell was used. Dosimetry was performed with  $\text{N}_2\text{O}$ -saturated 10 mM KSCN aqueous solution taking  $G_{(\text{OH})} = 6.0$  and  $\epsilon_{(\text{SCN})^{2-}} = 7600 \text{ M}^{-1} \text{ cm}^{-1}$  at 480 nm.<sup>22</sup>

## Results and Discussion

**1. Absorption and Fluorescence Spectra.** Figure 1 shows the absorption and fluorescence emission spectra of **2** in cyclohexane at 298 K. The absorption spectra show two bands, which are attributed to the  ${}^1\text{L}_{\text{b}} \leftarrow {}^1\text{A}$  and  ${}^1\text{L}_{\text{a}} \leftarrow {}^1\text{A}$  transitions.<sup>23</sup> The Stokes shifts ( $\Delta\nu$ ) are found to be similar (Table 1) for the aniline and for compound **2** in cyclohexane.<sup>23</sup> However, the larger Stokes shift in MeCN solution for compound **2** is an indication of the greater difference in dipole moment between the ground and excited state due to the partial charge-transfer character in the  $\text{S}_1$  state. The fluorescence quantum yields and fluorescence lifetimes were measured and are listed in Table 1. The fluorescence quantum yield of **2** decreases slightly on excitation into the  $\text{S}_2$  excited state ( $\lambda_{\text{ex}} = 254$  nm), an observation first made by Köhler and

(22) Jagannadham, V.; Steenken, S. *J. Am. Chem. Soc.* **1988**, *110*, 2188.

(23) Sarkar, S. K.; Kastha, G. S. *Spectrochim. Acta, Part A* **1992**, *48*, 1611.

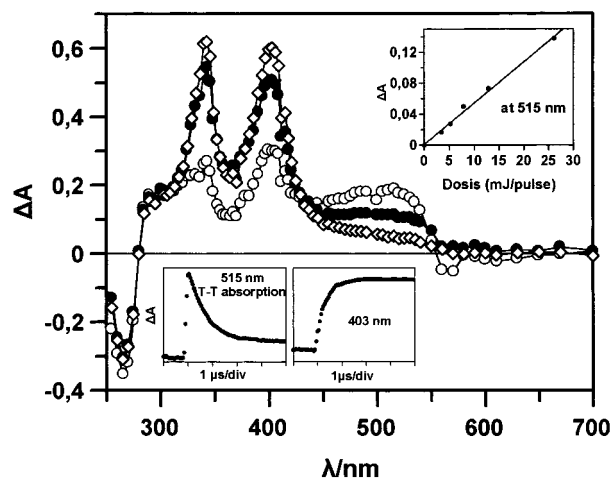
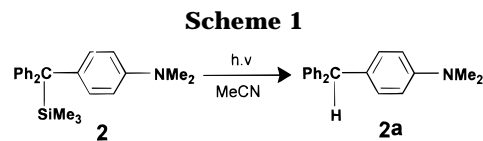


**Figure 2.** Time-resolved absorption spectra observed on 248-nm photolysis of an argon-saturated solution of **2** in hexane (0.076 mM). Spectra recorded at times (O) 30 ns, (●) 125 ns, and (◇) 375 ns after the pulse. Inset: yield of triplet state as a function of the laser power and time dependence of the optical density at 515 and 403 nm.

Getoff for aromatic amines<sup>21,24</sup> and attributed to photo-induced chemical transformations in the  $\text{S}_2$  state.

**2. Product Analysis.** Irradiation of an argon saturated solution of **2** in MeCN (0.1 mM) with the 248- and 308-nm laser light (15–100 shots) yields almost exclusively the desilylation product **2a** (Scheme 1) and traces of *p*-phenylaniline. The products were identified by GC and GC–MS through comparison with authentic samples. The desilylation product **2a** shows that the *p*-(dimethylamino)-triphenylmethyl radical (**3'**) might be an intermediate from which **2a** would be formed via hydrogen abstraction. Completely identical products were observed in MeOH as solvent.

**3. Laser Flash Photolysis Experiments. (a) Photolysis of **2** with 248- and 308-nm Laser Light in Hexane.** Photolysis of an argon saturated solution of **2** in hexane (0.076 mM) with 248-nm laser light produced the spectrum shown in Figure 2. The transient measured 30 ns after the pulse is characterized by a broad band in the region 420–560 nm with  $\lambda_{\text{max}}$  at 515 nm and two sharp peaks at 343 and 403 nm.

The broad band decays exponentially with a value  $k = 6.8 \times 10^6 \text{ s}^{-1}$  ( $\tau \approx 147$  ns, see Figure 2, inset), and its decay was accompanied by an increase of the two absorption bands at 343 and 403 nm, respectively ( $\tau_{\text{rise}} \approx 122$  ns, see Figure 2, inset). This transient is attributed to radical **3'**, which seems to be produced via the triplet state, since the buildup rate constant is similar to the decay of the triplet state. The presence of an isosbestic point (at ca. 440 nm) and the disappearance of both bands in the presence of oxygen atmosphere support further this assignment. The amplitude of the T–T absorption at 515-

(24) Köhler, G.; Getoff, N. *J. Chem. Soc., Faraday Trans. 1* **1980**, *76*, 1576. Köhler, G.; Rosicky, C.; Getoff, N. In *Excited States in Organic Chemistry and Biochemistry*; Pullman, B., Goldblum, N., Eds.; Reidel: Dordrecht, 1977; p 303.

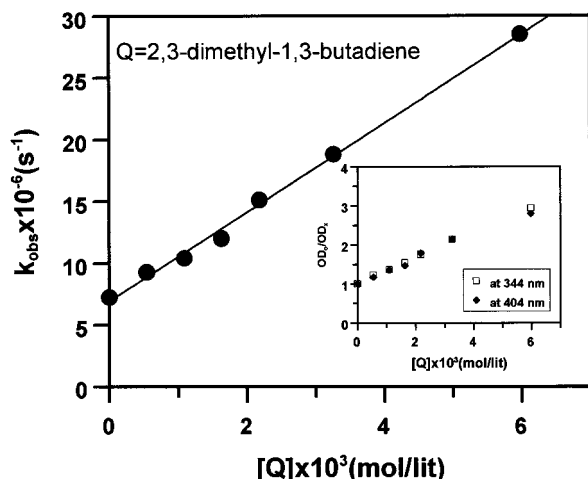


**Figure 3.** Quenching of the triplet state of **2** at 490 nm by 2,3-dimethylbuta-1,3-diene in cyclohexane (308-nm laser light). Inset: Stern–Volmer plot for the quenching of the radical production at 344 and 404 nm.

nm was found to increase linearly with the laser pulse power in the range 0–30 mJ (Figure 2, inset a). A linear dependence was found also for the radical formation, a fact that is in agreement with a radical formation via the triplet state.

To examine the photochemical behavior of this compound on excitation at the long wavelength absorption band, 308-nm laser light was used; the transient absorption spectra recorded in a deoxygenated hexane solution (0.2 mM) are identical to those obtained with 248-nm laser. The T–T absorption has a maximum at 510 nm, decays exponentially with a rate constant  $k = 7.5 \times 10^6 \text{ s}^{-1}$  (lifetime  $\tau = 133 \text{ ns}$ ), and its decay is followed by the formation of  $3^*$  ( $\lambda_{\text{max}}$  at 342 and 402 nm and  $\tau_{\text{rise}} \approx 119 \text{ ns}$ ).

The involvement of the triplet state was further confirmed by quenching experiments using typical quenchers such as 2,3-dimethylbuta-1,3-diene (Figure 3), styrene, and methyl methacrylate (we chose 308 nm laser light to avoid absorption from the quencher). The rate constant  $k_q$  was obtained as the slope of the plot of  $k_{\text{obs}}$  vs  $[Q]$  according to the simple relationship

$$k_{\text{obs}} = k_0 + k_q[Q]$$

where  $k_0$  is the observed first-order decay rate constant for the triplet state in the absence of quencher and  $k_{\text{obs}}$  is the observed rate constant in the presence of a given quantity of quencher  $[Q]$ , Figure 3. The  $k_q$  values obtained in cyclohexane (the absorption maximum of the triplet is a plateau at 490–520 nm) are  $3.6 \times 10^9 \text{ M}^{-1} \text{ s}^{-1}$  for 2,3-dimethylbuta-1,3-diene,  $4.1 \times 10^9 \text{ M}^{-1} \text{ s}^{-1}$  for styrene, and  $1.97 \times 10^9 \text{ M}^{-1} \text{ s}^{-1}$  for methyl methacrylate, comparable<sup>25</sup> to reported values for aniline or benzylaniline triplets. Also the radical formation measured at  $\lambda_{\text{max}} = 344$  and 404 nm obeys a similar Stern–Volmer relationship; see inset of Figure 3.

Using naphthalene as a triplet quencher and the known value  $\epsilon_{415} = 24\,500 \text{ M}^{-1} \text{ cm}^{-1}$  (quantum yield  $\Phi = 0.75$ ) for its triplet state,<sup>26</sup> assuming  $\Phi_F + \Phi_T = 1$  ( $\Phi_F = 0.075$ , see Table 1), we were able to calculate the molar

(25) Using 2,3-dimethylbuta-1,3-diene as a quencher, the values  $1.3 \times 10^{10} \text{ M}^{-1} \text{ s}^{-1}$  for aniline triplet<sup>16d</sup> and  $6.4 \times 10^9 \text{ M}^{-1} \text{ s}^{-1}$  for benzylaniline triplet<sup>8b</sup> were reported in hexane.

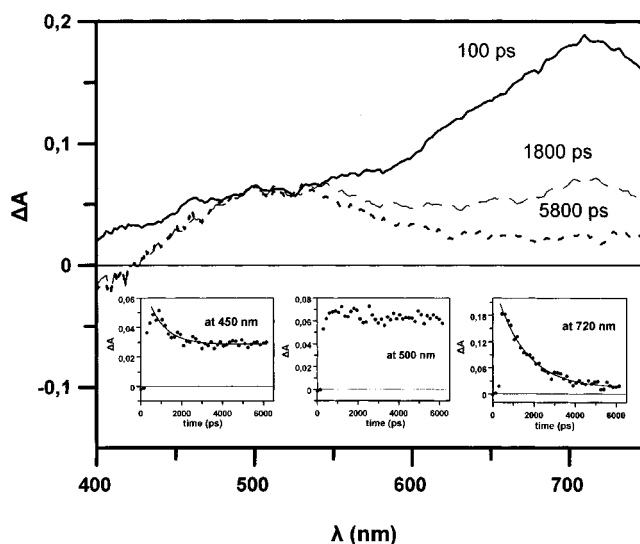


**Figure 4.** Time-resolved absorption spectra observed on picosecond 266-nm photolysis of **2** in cyclohexane. Spectra recorded at 100 ps (full line), 1800 ps (broken line), and 5800 ps (dotted line) after the pulse. Insets: time dependence of the optical density at 450, 500, and 720 nm, respectively.

extinction coefficient of the triplet state of **2** (following its absorption decay at 515 nm) as  $\epsilon_{515} = 4550 \text{ M}^{-1} \text{ cm}^{-1}$ , very close to that reported for PhNMe<sub>2</sub> ( $\epsilon_{460} = 4000 \pm 500 \text{ M}^{-1} \text{ cm}^{-1}$ ).<sup>27</sup> The existence of the isosbestic point at 440 nm (see Figure 2) indicates that the triplet state is converted exclusively to radical  $3^*$ , and under this condition, the quantum yield of the radical formation is  $\Phi_{3^*} = \Phi_T \approx 0.92$ . The dissociation efficiency of **2** is very high and similar to that of **1**.

**(b) Picosecond LFP with 266-nm Laser Excitation of 2 in Cyclohexane.** The involvement of the triplet state in the C–Si photodissociation of **2** is further demonstrated using 266-nm picosecond LFP. We obtained thus the spectra shown in Figure 4. The transient absorption measured at 100 ps after the exciting pulse is characterized by a broad band in the region 400–750 nm, peaking at 720 nm and showing a shoulder at ca. 510 nm. The absorption band at 720 nm decays exponentially with a rate constant  $k = 7.1 \times 10^8 \text{ s}^{-1}$  ( $\tau = 1400 \text{ ps}$ , see Figure 4, inset at 720 nm), while at 450 nm the decay rate is slower ( $\tau \approx 3600 \text{ ps}$ , see inset at 450 nm). Thus, after 4 ns the above absorption spectrum is replaced by a different absorption, having  $\lambda_{\text{max}} \approx 510 \text{ nm}$  and remaining constant at  $\tau > 8 \text{ ns}$ .

On the basis of the nanosecond LFP results, we assign the remaining absorption at 510 nm to the triplet state of **2**, which is long-lived and cannot be resolved with the ps apparatus ( $\tau \approx 148 \text{ ns}$  in hexane, see above). The transient corresponding to the 720 nm absorption and decaying with  $\tau = 1400 \text{ ps}$  is ascribable to the  $S_1$  state of **2** on the basis of the fluorescence lifetime reported above (1500 ps, Table 1). The  $S_1$  state intersystem crosses to the triplet state, a fact in accordance with the quantum yield  $\Phi = 0.92$  measured for the  $T_1$  formation on the ns time scale. The presence of a quasi isosbestic point around 500–520 nm (Figure 4 and inset at 500 nm) strengthens this interpretation, and a value of  $\epsilon_{720} \approx 15\,520 \text{ M}^{-1} \text{ cm}^{-1}$  can be calculated for  $S_1$  at 720 nm on

(26) Bensasson, E.; Land, E. J. *Photochem. Photobiol. Rev.* **1978**, 3, 163.

(27) Previtali, C. M. *J. Photochem.* **1985**, 31, 233.

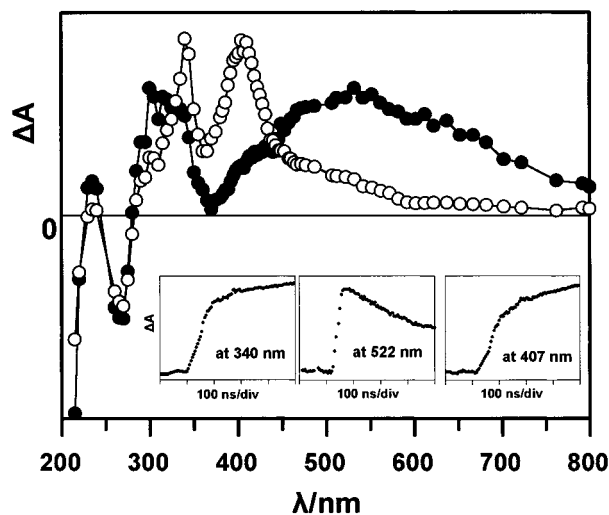


**Figure 5.** Time-resolved absorption spectra observed on 248-nm photolysis of an argon saturated solution of **2** in MeCN (0.11 mM). Spectra recorded at (●) 70 ns, (○) 750 ns, and (◆) 3  $\mu$ s after the pulse. Insets: time dependence of the optical density at 522, 340, and 407 nm, respectively.

the basis of  $\epsilon_{515} = 4550 \text{ M}^{-1} \text{ cm}^{-1}$  of the  $T_1$  reported above. Furthermore, on the basis of the quantum yield of formation of  $T_1$  and lifetime of  $S_1$ , the intersystem crossing rate constant  $k_{isc} \approx 6.6 \times 10^8 \text{ s}^{-1}$  is calculated, which is comparable to those obtained for other anilines.<sup>16c,d</sup>

**(c) Photolysis of **2** with 248- and 308-nm Laser Light in Acetonitrile.** Photolysis of an argon saturated solution of **2** in MeCN (0.1 mM) produced the spectrum shown in Figure 5. About 70 ns after the laser pulse a very broad intense absorption band in the 350–800 nm region with a maximum centered at  $\sim 530$  nm was recorded. A second band was observed at 300 nm. As these bands decayed, a new transient with maxima centered at 340 and 407 nm was formed. As can be seen in the inset of Figure 5, the rate constant for the decay of the band at 522 nm closely matches the rate constant for the growth of the new transient at 340 and 407 nm ( $k \approx 6 \times 10^6 \text{ s}^{-1}$ ).

When oxygen was admitted to the solution ( $[O_2] = 8.2 \text{ mM}$ ), a different transient spectrum was observed, see Figure 6; it consists of two absorption bands, one at 307 nm and a second broad band in the region of 400–800 nm. The latter has a maximum at  $\sim 640$  nm and a shoulder at  $\sim 450$  nm. The intense negative signal at 265 nm is attributed to the absorption band of the parent compound. A second very weak negative signal detected in the region 310–380 nm ( $\lambda_{max} \sim 350$  nm) within 25 ns after the pulse can be assigned to the fluorescence emission of the parent compound (see fluorescence data in Table 1 and Figure 1). The decay of the absorption at 307, 450 and 640 nm does not follow first-order kinetics but occurs on the same time scale (1.3  $\mu$ s), which means that the bands belong to the same transient. Almost the same value was calculated for the recovery of the negative signal at 265 nm (see inset in Figure 6), a fact indicating regeneration of the parent compound as a result of the decay of the transient. The transient with the two bands that appeared under argon at 340 and 407 nm was eliminated when oxygen was present and thus should belong to radical **3**\*, an assignment supported by the detection of **3**\* in hexane reported above.

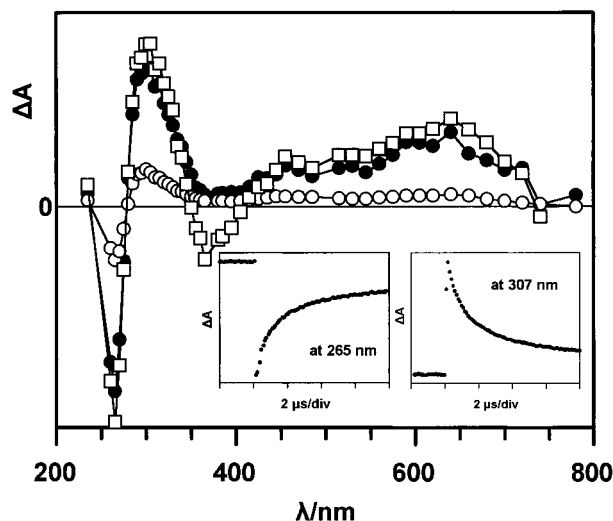


**Figure 6.** Time-resolved absorption spectra observed on 248-nm photolysis of an oxygen saturated solution of **2** in MeCN (0.1 mM). Spectra recorded at times (□) 25 ns, (●) 130 ns, and (○) 7  $\mu$ s, after the pulse. Inset: time dependence of the optical density at 265 and 307 nm.

It is also worth noting that under oxygen atmosphere the intensity of the broad band became smaller by at least 3 times and its decay became slower. The shape was changed, while the maximum was shifted from 530 to 640 nm. Consequently, under argon, the broad band should consist of at least two transient species: one with  $\lambda_{max}$  at 530 nm, which disappears under oxygen and therefore has a radical or triplet character, and a second one (640 nm), which was unaffected by  $O_2$  and probably possesses cationic character. On the basis of this behavior, the detection of the triplet state of **2** in hexane at  $\sim 515$  nm, and the independent generation of the radical cation **2**<sup>•+</sup> using pulse radiolysis (see below), we assign these transients to the triplet state of **2** and to **2**<sup>•+</sup>, respectively.

To study the photochemical behavior of **2** on excitation at the long wavelength band of the absorption, 308-nm laser light was used. Figure 7a shows the spectra recorded on irradiation of a 0.55 mM solution of **2** in MeCN 30, 150, and 700 ns after the pulse. They are similar with those produced by the 248-nm laser light. The broad band extending from 400 to 800 nm with  $\lambda_{max}$  at about 515 nm decays almost exponentially with a rate constant of  $4.2 \times 10^6 \text{ s}^{-1}$ . This transient was produced by a one-photon process, and its decay leads to the formation of **3**\* with maxima at 345 and 408 nm (rate constant of formation  $k = 4.1 \times 10^6 \text{ s}^{-1}$  at both wavelengths). Since these two absorption maxima also follow a monophotonic buildup and have the same kinetic profile as the transient at 515 nm, we can confidently assume that **3**\* is produced through the decay of this transient. The existence of an isosbestic point at 440 nm strengthens this assumption further.

The spectrum recorded in the presence of oxygen (Figure 7b) consists of a broad band in the range 400–800 nm with maximum at  $\sim 640$  nm (as in the case of 248-nm laser irradiation). This transient was produced by a two-photon process (see inset, Figure 7b) and was attributed to the corresponding radical cation.

**4. Pulse Radiolysis Experiments.** As already mentioned, the radical cation **2**<sup>•+</sup> is produced via photoionization of the parent compound in the polar solvent

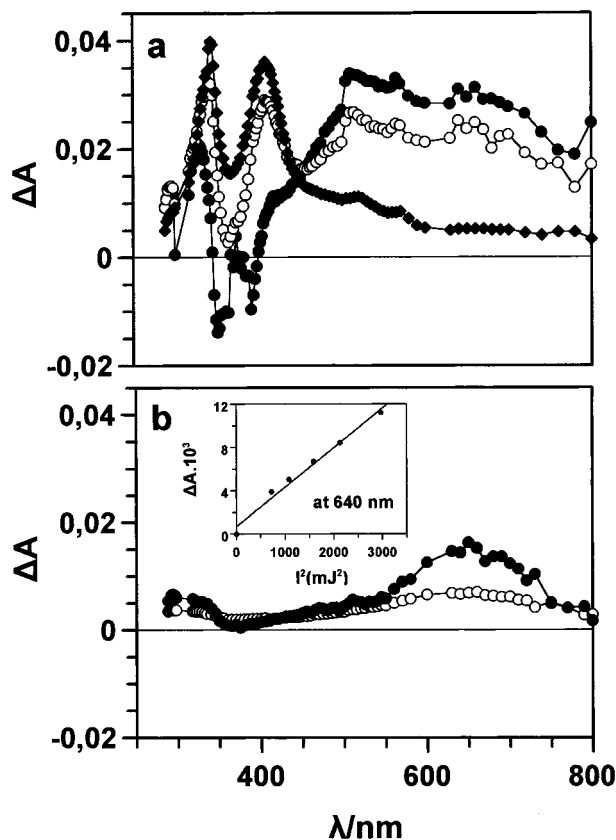
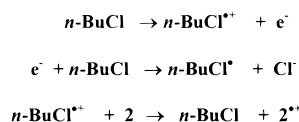


**Figure 7.** (a) Time-resolved absorption spectra observed on 308-nm photolysis of an argon saturated solution of **2** in MeCN (0.55 mM). Spectra recorded at times (●) 30 ns, (○) 150 ns, and (◆) 700 ns after the pulse. (b) Absorption spectra observed from the oxygen saturated solution (●) 300 ns and (○) 4  $\mu$ s after the pulse. Inset: photolysis of the transient at 640 nm immediately after the laser pulse.

#### Scheme 2



MeCN. To generate  $\mathbf{2}^{+\bullet}$  independently and to examine its fate, pulse radiolysis was used. This is a convenient method for generating radical cations. For this purpose *n*-BuCl was used as an appropriate solvent because of its ability to scavenge irreversibly the electrons produced by ionizing radiation, Scheme 2.<sup>28</sup>

The time-resolved absorption spectrum observed upon radiolysis of a 1.6 mM solution of **2** in *n*-BuCl in oxygen atmosphere is given in Figure 8. Two main absorption bands at 450 and  $\sim$ 650 nm and a shoulder at  $<$ 340 nm were observed 12.6  $\mu$ s after the pulse; their similar lifetime ( $\sim$ 32  $\mu$ s) implies that they belong to the same transient species. The similarity of this spectrum with the absorption spectra produced after photolysis of **2** (see Figures 6 and 7b) in oxygen atmosphere supports the assignment to  $\mathbf{2}^{+\bullet}$ . By conducting the experiment under argon the spectrum remains the same as expected for a radical cation, apart from a small additional absorption

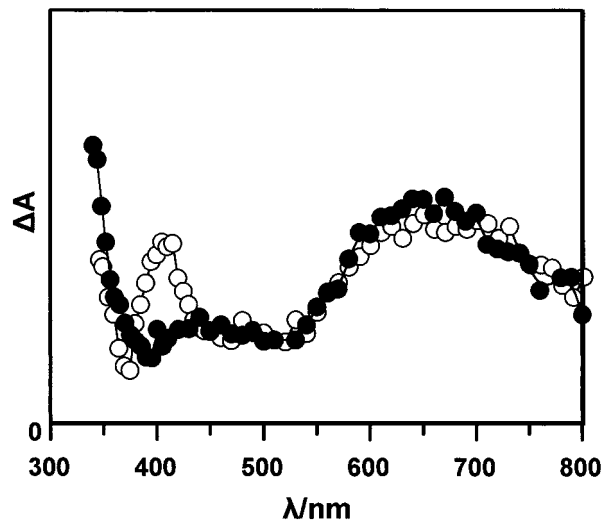


**Figure 8.** Transient absorption spectra observed on pulse radiolysis of an oxygenated (●) and a deoxygenated (○) 1.6 mM solution of **2** in *n*-BuCl, recorded at 12.6  $\mu$ s after the pulse.

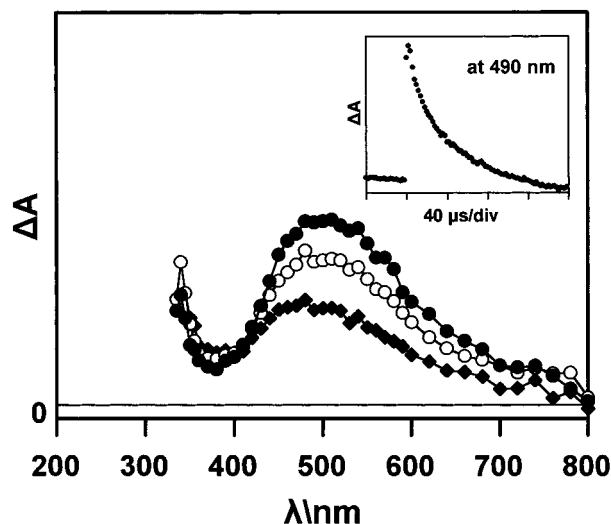
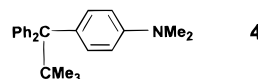


**Figure 9.** Transient absorption spectra observed on pulse radiolysis of an oxygenated 2.5 mM solution of **4** in *n*-BuCl. Spectra recorded at (●) 600 ns, (○) 4.4  $\mu$ s, and (◆) 14  $\mu$ s after the pulse. The inset shows the decay of the transient at 490 nm.

band appearing at  $\sim$ 405 nm that slightly increased as the radical cation  $\mathbf{2}^{+\bullet}$  decayed. This band is attributed to radical  $\mathbf{3}^{\bullet}$ , produced after desilylation of  $\mathbf{2}^{+\bullet}$ .

The red shift of the long wavelength absorption of  $\mathbf{2}^{+\bullet}$  ( $\sim$ 650 nm) relative to  $\text{PhN}^+\text{Me}_2$  (490 nm) is attributed to the hyperconjugative interaction of the benzylic Si–C bond with the delocalized system. Figure 9 shows the absorption spectrum obtained upon radiolysis of **4** in

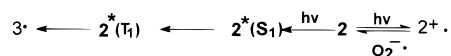


*n*-BuCl in oxygen atmosphere;  $\mathbf{4}^{+\bullet}$  thus produced shows a maximum at  $\sim$ 490 nm. Obviously, after replacing Si by carbon the bathochromic shift observed for  $\mathbf{2}^{+\bullet}$  is eliminated.

**5. EPR Spectroscopy.** Irradiation of a solution of **2** in various solvents (hexane, diethyl ether, dioxane, benzene) with a low-pressure lamp (Heraeus TNN-15W,

(28) Sprinks, J. W. T.; Woods, R. J. *An Introduction to Radiation Chemistry*; Wiley-Interscience: New York, 1976; p 396. Adam, W.; Kammel, T.; Toubartz, M.; Steenken, S. *J. Am. Chem. Soc.* **1997**, *119*, 10673.

## Scheme 3



emission at 254 nm) produces a very stable and highly resolved EPR spectrum with  $g$  value 2.0027, characteristic of carbon centered radicals.<sup>29</sup> A complete analysis of the spectrum was not performed.

**6. Conclusions.** We have shown that on irradiation in MeCN **2** undergoes photodissociation and photoionization to **3** $\cdot$  and **2** $^{+\cdot}$ , respectively (Figure 5–7 and Scheme 3). Very probably the formation of **3** $\cdot$  takes place from the triplet state, which is produced monophotonically, while that of **2** $^{+\cdot}$  is a two-photon process. In a subsequent step, **2** $^{+\cdot}$  is reduced back to the parent compound **2** (Figure 6), probably through return electron transfer with superoxide anion  $O_2^-$ , as has been also found previously for the benzyltriisopropylsilane radical cation:<sup>18b</sup> while  $PhCH_2SiMe_3^{+\cdot}$  undergoes desilylation via nucleophile-assisted C–Si bond cleavage (with MeCN acting as a nucleophile) and gives  $PhCH_2\cdot$  radical,  $PhCH_2Si(i-Pr)_3^{+\cdot}$ , being more sterically hindered, prevents a similar nucleophilic attack and leads through return electron transfer with  $O_2^-$  to the regeneration of the parent  $PhCH_2Si(i-Pr)_3$ .<sup>18a,b,g</sup>

In the case of **2** $^{+\cdot}$  the even more demanding steric constraints of the triphenylmethyl group (relative to  $Si(i-Pr)_3$ ) prevent an analogous nucleophilic attack by the solvent (MeCN) and thus lead to a regeneration of **2** (Scheme 3) and not to **3** $\cdot$ . This is more surprising since the C–Si bond strength in **2** $^{+\cdot}$  must be much lower than that in  $PhCH_2SiMe_3^{+\cdot}$ . The above conclusion appears to be in contradiction to the pulse radiolysis results, where **2** $^{+\cdot}$  gives to some extent **3** $\cdot$ ; this fact is, however, not unexpected if we consider the presence of a better and smaller nucleophile  $Cl^-$  produced by the pulse radiolysis experiment.

A further support for the above findings stems from the behavior of **4** $^{+\cdot}$ ; here a nucleophile-assisted C–C bond cleavage with subsequent formation of **3** $\cdot$  is unlikely.<sup>17e</sup> Radical cation **4** $^{+\cdot}$ , produced in MeCN through 248-nm photolysis (Figure 10), show decay rate constant at 285 and 515 nm (early decay time  $1.1 \times 10^6$  s $^{-1}$ ; inset b,c) similar to the rate of regeneration of **4** at 265 nm ( $1.3 \times 10^6$  s $^{-1}$ ; inset a). When the experiment is conducted under argon, no formation of **3** $\cdot$  from **4** $^{+\cdot}$  has been observed. Similar results we obtained also by the 248-nm photolysis of **4** in *i*-PrOH/H<sub>2</sub>O (1/1).

In hexane where the photoionization pathway is absent (Figure 2), the involvement of the triplet state in the formation of **3** $\cdot$  is clearly demonstrated. The triplet state decays with the same rate constant as the formation of **3** $\cdot$  (isosbestic point at 440 nm), and both follow a linear Stern–Volmer plot (Figure 3) with 2,3-dimethylbuta-1,3-diene as a quencher. Furthermore, using picosecond LFP (Figure 4) we were able to detect the  $S_1$  state of **2**, which was found to absorb at  $\lambda_{max} \approx 720$  nm. The latter shows a lifetime  $\tau = 1400$  ps, close to the fluorescence lifetime

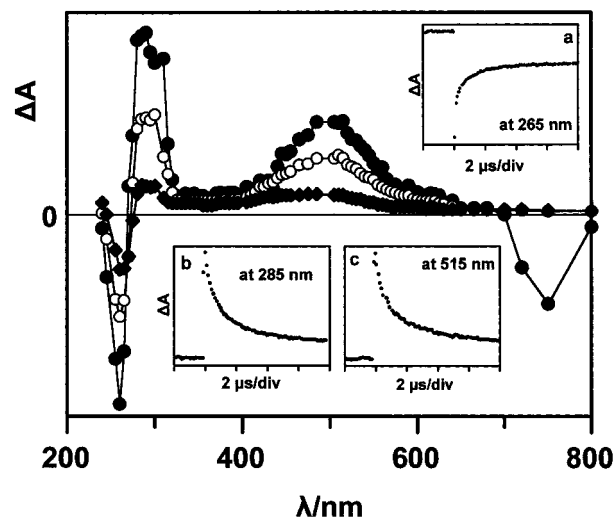


**Figure 10.** Time-resolved absorption spectra observed on 248-nm photolysis of a saturated with oxygen 0.1 mM solution of **4** in MeCN. Spectra recorded at times (●)125, (○)700, and (◆)7.5  $\mu$ s after the pulse. Insets: time dependence of the optical density at 265, 285, and 515 nm, respectively.

$\tau_f = 1500$  ps, and is converted almost exclusively to the  $T_1$  state ( $\Phi_T = 0.92$ ). The  $T_1$  state is persistent on the ps time scale. The whole sequence of events  $2 \rightarrow S_1 \rightarrow T_1 \rightarrow 3\cdot$  is thus clearly elucidated in nonpolar solvents such as hexane or cyclohexane.

EPR spectroscopy also supports the above conclusions. Photolyzing **2**, we recorded a highly resolved EPR spectrum that corresponds to a carbon-centered radical of the trityl type.

## Summary

In polar media like MeCN, **2** undergoes photoionization to the radical cation **2** $^{+\cdot}$  in a two-photon process and in part dissociates to the radical **3** $\cdot$  via the triplet state. The bulkiness of the triphenylmethyl group obviously prevents the dissociation of **2** $^{+\cdot}$  via a nucleophile-assisted C–Si cleavage to **3** $\cdot$ . In nonpolar solvents such as hexane or cyclohexane, only the second process takes place, leading to **3** $\cdot$  in high quantum yield ( $\sim 0.92$ ); the complete sequence  $2 \rightarrow S_1 \rightarrow T_1 \rightarrow 3\cdot$  is elucidated using ns and ps LFP. Despite the high dissociation quantum yield, the high quenching rate constants of the triplet state of **2** by styrene ( $k_q = 4.1 \times 10^9$  M $^{-1}$  s $^{-1}$ ) and methyl methacrylate ( $1.97 \times 10^9$  M $^{-1}$  s $^{-1}$ ) compared to the photodissociation rate constant  $6.8 \times 10^6$  s $^{-1}$  renders questionable its potential as a photoinitiator with these two monomers. Work is in progress hereupon.

**Acknowledgment.** We thank Bundesministerium für Forschung und Technologie (Germany) and General Secretariat for Research and Technology (Greece) for a grant (6BOA1A). We thank also Dr. G. Gurzadyan for the ps measurements and Dr. J. Leitich and Dr. M. Canle for reading the draft. A.K.Z. thanks the Deutscher Akademischer Austauschdienst for a fellowship (1998).

(29) Neumann, W. P.; Uzick, W.; Zarkadis, A. K. *J. Am. Chem. Soc.* **1986**, *108*, 3762.